Progress In Electromagnetics Research, *PIER 12, 37–56, 1996*

DIFFERENCES BETWEEN MODAL EXPANSION AND INTERGRAL EQUATION METHODS FOR PLANAR NEAR-FIELD TO FAR-FIELD TRANSFORMATION

P. Petre and T. K. Sarkar

1. Introduction

Near field antenna measurements are widely used in antenna testing since they allow for accurate measurements of antenna patterns in a controlled environment. The earliest works are based on the modal expansion method in which the fields radiated by the test antenna are expanded in terms of planar, cylindrical or spherical wave functions and the measured near fields are used to determine the coefficients in the expansion [1–4]. In this paper, we focus our attention primarily on planar near field measurements. A problem of the planar modal expansion technique is that the fields outside the measurement region are assumed to be zero. This assumption results in a systematic error in the computations involved in the planar modal expansion theory. If the measurement plane is of dimension $L \times L$ and the source plane (the plane which encompasses the sources) is of dimension $D \times D$, then the planar modal expansion theory holds up to an angle θ, which is given by $\theta = \tan^{-1}\left(\frac{L-D}{2d}\right)$, where d is the separation distance between the two planes as shown in Fig. 1 [5].

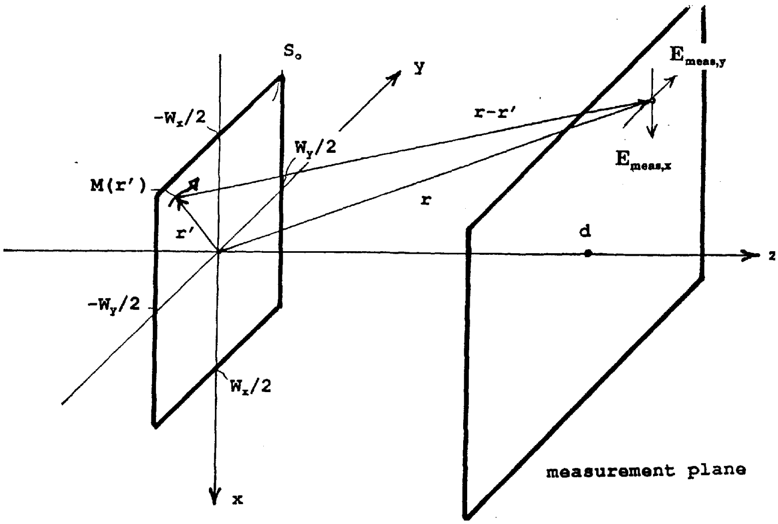

Figure 1. Planar near-field measurement.

An alternate method of computing far-fields from measured near-fields has recently been explored [6,7] utilizing an equivalent magnetic current approach. This method utilizes the measured near field data obtained on the $L \times L$ measurement plane to determine equivalent currents on the $D \times D$ source plane which encompass all sources as mentioned earlier. These equivalent currents may then be used to image the sources on the antenna if desired (for fault diagnosis) and also to compute the far fields. This is in distinction to the planar modal expansion method where the far fields are computed first and then they are Fourier transformed to the source plane to image the sources [8].

The objective of this paper is to demonstrate that: (A) when the measurement plane is infinite the planar modal expansion technique and the integral equation technique provide the same analysis equations. It will be shown that in that case the planar modal expansion solves the integral equation in the spectral domain whereas the newly developed equivalent current approach solves the problem in the space domain. (B) The truncation error in the equivalent current approach is smaller as one transfers the data from the measurement plane to the source plane before Fourier transforming it to compute the far fields. Hence, the results for the equivalent current approach should hold over a larger azimuth angle θ than the planar modal expansion method.

Section 2 describes the planar modal expansion method. Section 3 presents the equivalent current approach. Section 4 shows the equivalence between the two techniques. Limited numerical results are presented in Section 5 based on both numerically simulated data and experimental data.

2. Modal Expansion Method

For the modal expansion method, two components of the electric field E_x and E_y are measured on the measurement plane, which is at a distance d from another plane located at $z = 0$, which is referred to as the source plane. All the sources are assumed to be behind this source plane as shown in Fig. 1, i.e. $z \leq d$. The sources may not be planar sources. The measured fields are $E_{meas,x}$ and $E_{meas,y}$ at the measurement plane. Since an equivalent magnetic current on a plane is related to the tangential components of the electric fields, then one could say that on the measurement plane there are two equivalent magnetic currents, as

$$\vec{M} = \vec{E} \times \vec{n} \tag{1}$$

where $\vec{n}$ is the direction of the outward normal on the measurement plane. This results in

$$M_y = -E_{meas,x} \tag{2}$$

$$M_x = E_{meas,y} \tag{3}$$

two magnetic current sheets located at $z = d$. The far field from the two magnetic current sheets can be evaluated as [9]

$$E_{far,x}(r, \theta, \phi) = jk_0 \cos\theta \, \frac{e^{-jk_0 r}}{4\pi r} \iint_{-\infty}^{\infty} M_y\left(x', y', z' = d\right) e^{+j\vec{k}\cdot\vec{r}'} \, dx' dy' \tag{4}$$

where

$$\begin{aligned}\vec{k}\cdot\vec{r}\,' &= k_0\sin\theta\cos\phi\, x' + k_0\sin\theta\sin\phi\, y' + k_0\cos\theta\, z' \\ &= x'k_x + y'k_y + z'k_z \qquad (5)\end{aligned}$$

where ${k_0}^2 = {k_x}^2 + {k_y}^2 + {k_z}^2 = (2\pi / \lambda_0)^2$ is the free space wavelength. The y-component of the far field is given by

$$E_{far,y}(r,\theta,\phi) = -jk_0\cos\theta\,\frac{e^{-jk_0 r}}{r}\iint_{-\infty}^{\infty} M_x(x',y',z'=d)\,e^{j\vec{k}\cdot\vec{r}'}\,dx'dy' \qquad (6)$$

If we consider $\tilde{M}_x(k_x,k_y,z'=d)$ to be the two dimensional Fourier transform of $M_x(x',y',z'=d)$, then

$$\tilde{M}_x(k_x,k_y,z'=d) = \iint_{-\infty}^{\infty} M_x(x',y',z'=d)\,e^{j(x'k_x+y'k_y)}\,dx'dy' \qquad (7)$$

and

$$\tilde{M}_y(k_x,k_y,z'=d) = \iint_{-\infty}^{\infty} M_y(x',y',z'=d)\,e^{j(x'k_x+y'k_y)}\,dx'dy' \qquad (8)$$

Under (7) and (8), (4) and (6) become

$$E_{far,x}(r,\theta,\phi) = C\cos\theta\tilde{M}_y(k_x,k_y,z'=d)\,e^{j\sqrt{{k_0}^2-{k_x}^2-{k_y}^2}\,d} \qquad (9)$$

$$E_{far,y}(r,\theta,\phi) = C\cos\theta\tilde{M}_x(k_x,k_y,z'=d)\,e^{j\sqrt{{k_0}^2-{k_x}^2-{k_y}^2}\,d} \qquad (10)$$

where C is some constant dependent on the parameter k_0.

If we consider $m_x(x',y',z'=0)$ and $m_y(x',y',z'=0)$ be two planar equivalent current sheets at the source plane $z=0$, then $\tilde{m}_x(k_x,k_y,z'=0)$ and $\tilde{m}_y(k_x,k_y,z'=0)$ will be their respective two dimensional Fourier transforms.

In that case

$$E_{far,x}(r,\theta,\phi) = C\cos\theta\tilde{m}_y\left(k_x,k_y,z' = 0\right) \tag{11}$$
$$E_{far,y}(r,\theta,\phi) = C\cos\theta\tilde{m}_x\left(k_x,k_y,z' = 0\right) \tag{12}$$

Hence the equivalent magnetic currents at the source plane and on the measurement plane are related in the spectral domain by

$$\tilde{m}_y\left(k_x,k_y,z'=0\right) = \tilde{M}_y\left(k_x,k_y,z'=d\right)e^{j\sqrt{{k_0}^2-{k_x}^2-{k_y}^2}\,d} \tag{13}$$
$$\tilde{m}_x\left(k_x,k_y,z'=0\right) = \tilde{M}_x\left(k_x,k_y,z'=d\right)e^{j\sqrt{{k_0}^2-{k_x}^2-{k_y}^2}\,d} \tag{14}$$

Therefore to image the source plane, in the conventional planar modal expansion one takes the two dimensional fourier transform of the measurement data to go to the far field and then the far field is directly related to the equivalent currents on the source plane by the inverse Fourier transform. The problem and the solution procedure is exact and no approximation is involved.

However, the problem is due to natural constraints. The limits for the double integrals in (4) and (6) are no longer infinity but finite. If the measurement plane is finite, then while taking the Fourier transforms of (4)–(8) it is clear that many of the relationship will be only approximate! The question is: under the constraint that the dimension of the measurement plane is finite which set of magnetic currents provide more accurate results for the far fields? Are they provided by $\tilde{M}_x$ and $\tilde{M}_y$ or by $\tilde{m}_x$ and $\tilde{m}_y$?

If the nonplanar sources are located behind the source plane and assuming Huygen's principle to hold, the source plane would capture more of the energy in the fields than the measurement plane if they are assumed to be of the same dimensions. This is because if the measurement plane, which is of the same dimension as the source plane, is situated an additional distance d away from the sources it has to intercept less of the fields. Hence the magnetic currents represented by M_x and M_y has a larger truncation error than m_x and m_y.

It is our intent to show that the integral equation approach utilizing the equivalent magnetic current approach solves for $m_x\left(x',y',z' = 0\right)$ and $m_y\left(x',y',z' = 0\right)$ and then performs a two dimensional Fourier transform to find the far fields.

To find E_θ and E_ϕ, the z-component of the electric field is also required. However, it is found from the divergence equation. Since in a source free region,

$$\bar{\nabla} \cdot \bar{E} = \frac{\partial E_x}{\partial x} + \frac{\partial E_y}{\partial y} + \frac{\partial E_z}{\partial z} = 0 \tag{15}$$

If $\tilde{E}_z(k_x, k_y)$ denote the two dimensional Fourier transform of $E_z(x', y')$ then

$$\tilde{E}_z(k_x, k_y) = -\frac{k_x \tilde{E}_x(k_x, k_y) + k_y \tilde{E}_y(k_x, k_y)}{k_z} \tag{16}$$

and from (5)

$$k_z = \sqrt{{k_0}^2 - {k_x}^2 - {k_y}^2} \tag{17}$$

So once $\tilde{E}_z(k_x, k_y)$ is known from (16), the far fields are given by

$$E_\theta = E_{far,x} \cos\theta \cos\phi + E_{far,y} \cos\theta \sin\phi - E_{far,z} \sin\theta \tag{18}$$

$$E_\phi = -E_{far,x} \sin\phi + E_{far,y} \cos\theta \tag{19}$$

In the next section we look at the integral equation approach utilizing the equivalent magnetic current.

3. Integral Equation Approach

For the integral equation approach, a fictitious source plane is considered of the same dimension as the measurement plane but translated a distance d towards the sources. So the source plane is located at $z' = 0$. As outlined in [7] an equivalent magnetic current of strength $2m$ is placed on the source plane at $z = 0$. The factor of 2 arises due to the application of the equivalence principle to a magnetic current radiating in the presence of a perfectly conducting ground plane. On this source plane, we put fictitious magnetic currents. The basic philosophy here is that if one knows the complex values of the magnetic currents on the source plane, one can evaluate the fields at the measurement plane. Conversely, if the measurement fields are known, then one can find the complex amplitudes of the magnetic currents m put on the source plane mathematically.

$$E_{meas,x} = \iint_{-\infty}^{\infty} 2m_y(x', y', z' = 0) \frac{\partial G(r, r')}{\partial z'} dx'dy' \tag{20}$$

$$E_{meas,y} = \iint_{-\infty}^{\infty} 2m_x(x', y', z' = 0) \frac{\partial G(r, r')}{\partial z'} dx'dy' \tag{21}$$

where $G(r, r')$ is the free space Green's function. The explicit expression is:

$$\frac{\partial G(r, r')}{\partial z'} = \frac{e^{-jk_0|\bar{r}-\bar{r}'|}}{4\pi|\bar{r}-\bar{r}'|^2}(z - z')\left[jk_0 + \frac{1}{|\bar{r}-\bar{r}'|}\right] \tag{22}$$

where $|\bar{r} - \bar{r}'|$ is the distance between the source point and the field point. Observe here, $z' = 0$ and $z = d$.

Now if we take the two dimensional Fourier Transform of both sides, this results in

$$\iint_{-\infty}^{\infty} E_{meas,x}(x, y, z = d)\, e^{j(k_x x + y k_y)} dxdy = 2\tilde{m}_y(k_x, k_y)\, \tilde{g}(k_x, k_y) \tag{23}$$

where $\tilde{m_y}$ is the two dimensional Fourier Transform of the magnetic currents located at the source plane and $\tilde{g}$ is two dimensional Fourier transform of the derivative of the Green's function

$$\tilde{G}(k_x, k_y, z, z') = \frac{-j}{2k_0} e^{j|z-z'|\sqrt{{k_0}^2 - {k_x}^2 - {k_y}^2}} \tag{24}$$

with

$$\text{Re}\left\{\sqrt{{k_0}^2 - {k_x}^2 - {k_y}^2}\right\} \geq 0 \tag{25}$$

and

$$\text{Im}\left\{\sqrt{{k_0}^2 - {k_x}^2 - {k_y}^2}\right\} < 0 \tag{26}$$

In the transform domain, the derivative of the spectral Green's function with respect to z' yields:

$$\frac{\partial}{\partial z'} \tilde{G}(k_x, k_y, z, z') = \frac{1}{2}\text{sgn}(z - z')\, e^{j|z-z'|\sqrt{{k_0}^2 - {k_x}^2 - {k_y}^2}} \tag{27}$$

where sgn(z) is the signum function. Since $z' = 0$ and $z = d$

$$\tilde{g}\left(k_x, k_y\right) = \frac{1}{2}\, e^{-jd\sqrt{{k_0}^2 - {k_x}^2 - {k_y}^2}} \tag{28}$$

Utilizing (21) and (26) and comparing it with (4) and (5) it becomes clear that

$$\tilde{M}_y\left(k_x, k_y, z = d\right) = \tilde{m}_y\left(k_x, k_y, z = 0\right) e^{-jd\sqrt{{k_0}^2 - {k_x}^2 - {k_y}^2}} \tag{29}$$

and

$$\tilde{M}_x\left(k_x, k_y, z = d\right) = \tilde{m}_x\left(k_x, k_y, z' = 0\right) e^{-jd\sqrt{{k_0}^2 - {k_x}^2 - {k_y}^2}} \tag{30}$$

Hence (27) and (28) are equivalent to (13) and (14). So if the information on the measurement plane were available, then the integral equation approach is basically to transfer the measurement data to the source plane and then take the Fourier transform to the far field. However, if the measurement plane is finite in size then the transfer of the data from $z = d$ plane to $z = 0$ plane utilizing the Fourier transform is not accurate because of the truncation error. Therefore we utilize an alternate transformation to go to the source plane. This alternate transformation is utilized in the integral equation approach through the utilization of the Green's function. Theoretically, this reduces the truncation error problem introduced by the two dimensional Fourier transform.

When the measurement plane is finite in nature then (29) and (30) do not hold and one has to use (20) and (21) to solve for m_x and m_y. The classical method of moments has been utilized to solved for m_x and m_y. The unknowns are replaced by elementary dipoles. This is a good approximation as long as the source and the measurement planes are separated by a wavelength (i.e. $d = \lambda$) [11]. Secondly, the use of dipoles eliminates the need for integration of the matrix elements in the evaluation of the impedance matrix. The two decoupled equations (20) and (21) are solved as the two matrix equations:

$$\left[E_{meas,x}\right] = \left[Z_{yx}\right]\left[m_y\right] \tag{31}$$

$$\left[E_{meas,y}\right] = \left[Z_{xy}\right]\left[m_x\right] \tag{32}$$

These matrices can be very large. However the equations can be solved very efficiently utilizing the FFT and the conjugate gradient method as outlined in [7]. Also the solution of (31) and (32) are decoupled and can be done simultaneously. Typically for 6400 unknowns for m_x or m_y the number of iterations taken to provide acceptable solution is about 10.

Since per iteration, two two-dimensional FFT is computed, the integral equation method is about 20 times slower than the modal expansion method for 6400 unknowns. Typically on a VAX workstation this amounts to a few seconds of CPU time for the modal expansion method as compared to several minutes of CPU time for the integral equation method to solve for the unknown magnetic currents m_x and m_y at the source plane. Once these magnetic currents are known, the far field can easily be computed utilizing the FFT.

4. Numerical Examples

In this section, we consider a theoretical simulation and a second example utilizing experimental data.

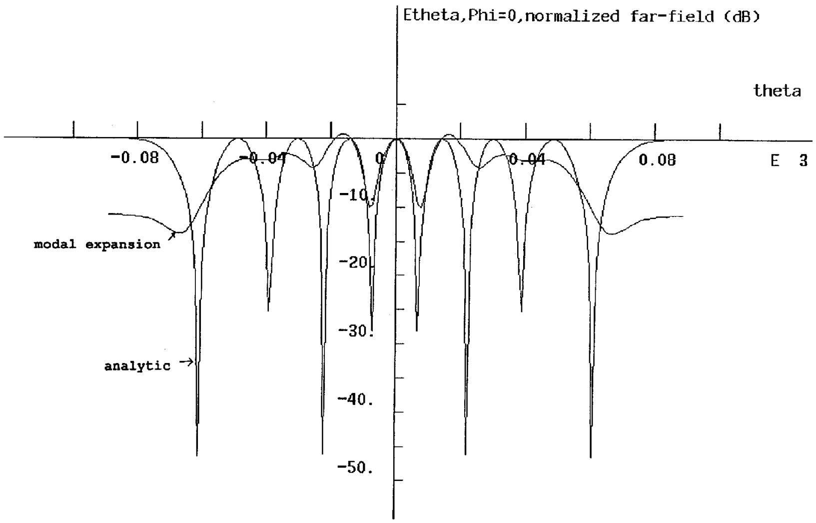

Figure 2. Comparison of exact and computed far-fields for $\Phi = 0$ cut for 2×2 magnetic dipoles on a $4\lambda \times 4\lambda$ surface using modal expansion method.

As a first example consider an array of 4 x-directed magnetic Hertzian dipoles placed on the corners of a $4\,\lambda$ by $4\,\lambda$ planar surface. This is considered as the test antenna. The measurement plane is considered $4.5\,\lambda$ by $4.5\,\lambda$ situated at a distance of $3\,\lambda$ from the source plane. Near fields are computed at 15 equispaced points of $0.3\,\lambda$ spacing (i.e. $\delta x = \delta y = 0.3\lambda$). Utilizing the planar modal expansion to compute the far field will be equivalent to taking the 2-dimensional Fourier transform of the 15×15 points. The normalized far fields $E_\theta(\phi = 0)$ and $E_\phi(\phi = 90°)$ for various values of θ are presented in Figs. 2 and 3.

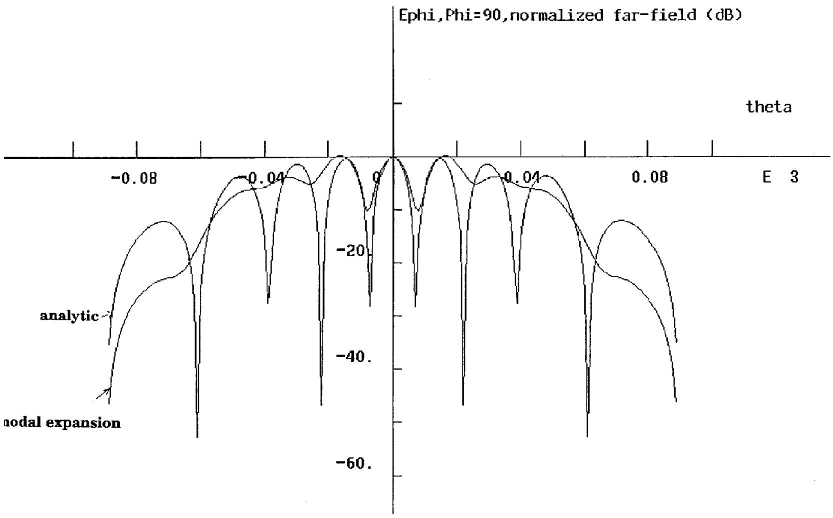

Figure 3. Comparison of exact and computed far-fields for $\Phi = 90$ cut for 2×2 magnetic dipoles on a $4\lambda \times 4\lambda$ surface using modal expansion method.

As expected the accuracy of the planar modal expansion will be valid up to $\tan^{-1}\left(\frac{0.25}{3}\right) \approx 10°$ [5]. The numerical simulations do illustrate that the calculated values for the far fields are acceptable up to $\pm 12°$.

For the integral equation approach, 15×15 magnetic dipole sources were considered at the source plane $z = 0$. The amplitudes of the 15×15 dipole sources were computed utilizing the integral equation approach utilizing magnetic currents for the same data over the 15×15 grid in the measurement plane. The 2D Fourier transform is then taken to find the far fields. The results are given in Figs. 4 and 5. Figure 4 provides $E_\theta\,(\phi = 0)$ and Fig. 5 describes $E_\theta\,(\theta = 90°)$ for various angles of θ.

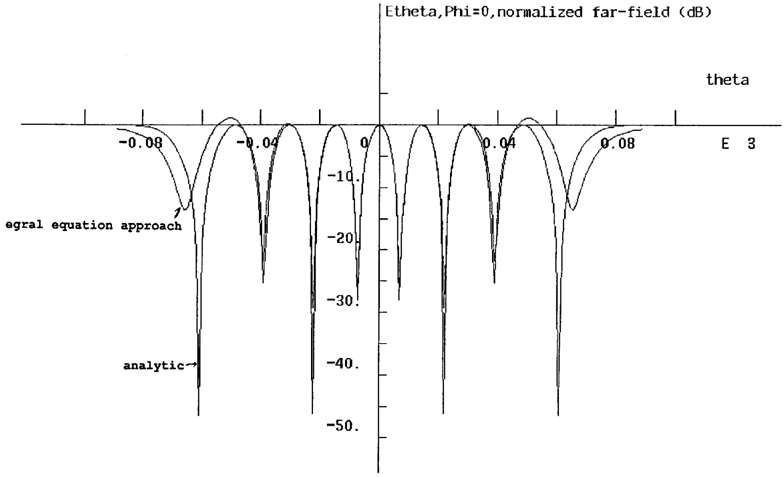

Figure 4. Comparison of exact and computed far-fields for $\Phi = 0$ cut for 2×2 magnetic dipoles on a $4\lambda \times 4\lambda$ surface using integral equation method.

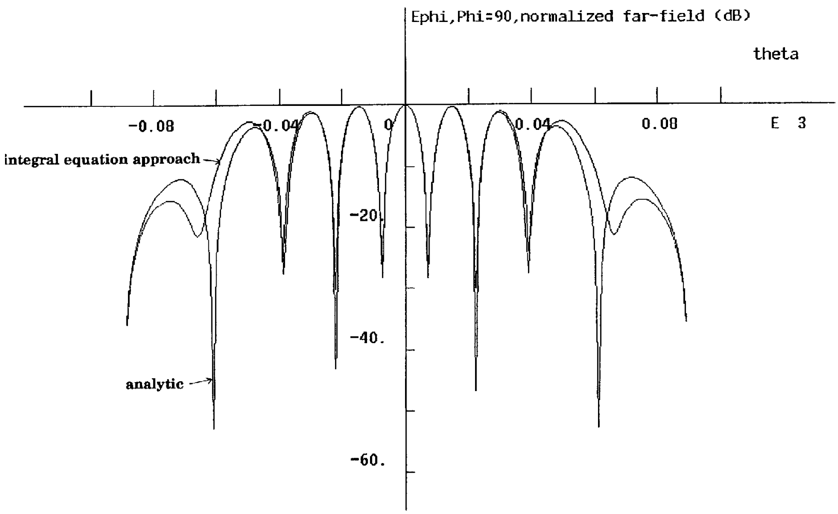

Figure 5. Comparison of exact and computed far-fields for $\Phi = 90$ cut for 2×2 magnetic dipoles on a $4\lambda \times 4\lambda$ surface using integral equation method.

It is seen for this case the calculated far fields are accurate up to $\pm 50^\circ$. This is because the truncation error is reduced by transforming the measured fields to an equivalent plane much closer to the sources as discussed in the earlier section.

As a second example, we consider experimental data for a microstrip array. This microstrip array consists of 32×32 uniformly distributed dipoles over a 1.5m $\times$ 1.5m surface. The operating frequency is 3.3 GHz. The array is considered in the $x - y$ plane. The x and y components of the electric near fields are measured on a plane 3.24m $\times$ 3.24m at a distance of 35cm from the array. There are 81×81 measured points at a distance of 4cm apart. This planar near field data was provided by Dr. Carl Stubenrauch of NIST [10].

If the planar modal expansion method is applied on the 81×81 measured data points, the computed far field will be accurate up to $\tan^{-1}\left(\frac{87}{35}\right) \approx 68^\circ$ [5]. The results obtained using modal expansion method were compared with the integral equation method as outlined in [7]. In [7], it was seen that the agreement between the two methods were good up to $\pm 60^\circ$ and acceptable in the rest of the elevation range.

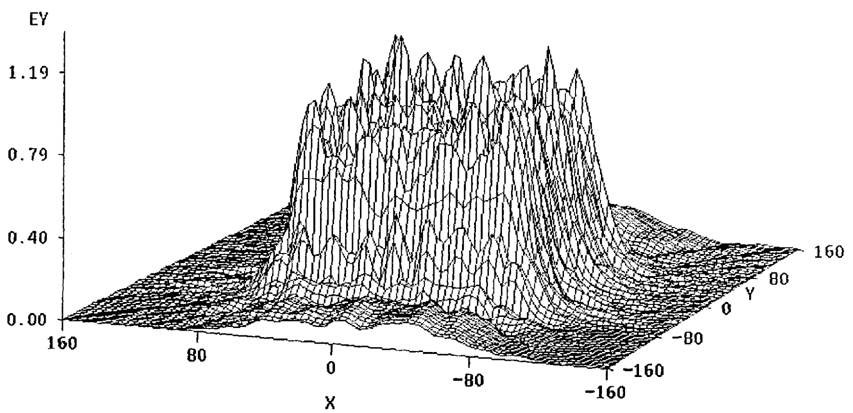

Figure 6. Amplitude of y component of measured electric near-field for a 32×32 patch microstrip array.

To demonstrate that by transferring the measured data to a fictitious surface, we are indeed reducing the truncation error, we take only 41×41 samples discarding 75% of the data. Therefore, we are considering the data only over a 1.64m $\times$ 1.64m measurement plane. By observing the magnitudes of the two components of the electric field (namely E_y in Fig. 6 and E_x in Fig. 7. The amplitude of the normalization component for E_x is 23.8 dB below that for E_y) it is clear that taking 41×41 points introduces significant truncation error if we were to take the direct Fourier transform of the data in the conventional modal expansion method. The Figs. 6 and 7 are for all the 81×81 data points. Hence by considering only 41×41 data points in Figs. 6 and 7, one is incurring a large truncation error in the conventional modal expansion method.

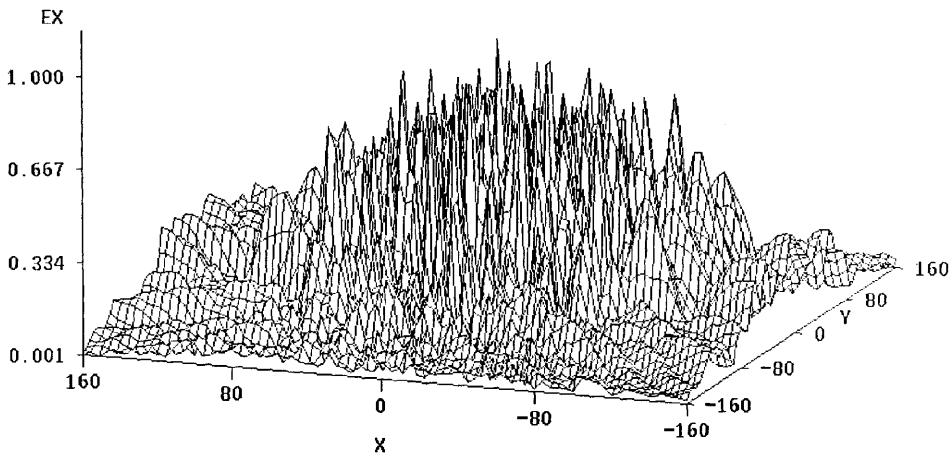

Figure 7. Amplitude of x component of measured electric near-field for a 32×32 patch microstrip array.

If the modal expansion method is applied to the 41×41 data points, the calculated far fields would be accurate upto $\tan^{-1}\left(\frac{7}{35}\right) \approx 11.3^\circ$. For the integral equation approach, we consider a 41×41 magnetic dipole array uniformly distributed over a 1.64m $\times$ 1.64, surface at the $z = 0$ plane. From the 41×41 measured near-field sampled data, we compute the amplitudes of the 41×41 magnetic dipoles utilizing CGFFT [7].

The $2D$ Fourier transform was then utilized to find the far fields. Figure 8 provides $E_\phi\,(\phi = 0)$ utilizing the modal expansion method with the original 81×81 points and the integral equation approach with only 41×41 data points.

It is seen that for the two results agree till $\pm 40^\circ$ and beyond that the agreement is reasonable. Therefore, by reducing the data by as much as 75% it is still possible to get reasonable results utilizing the integral equation technique. For this case 41×41 data points, the CGFFT method takes about 10–12 iterations to provide an acceptable solution for the magnetic dipoles. Since the CGFFT method requires two 2D-FFT per iteration, the CGFFT method is slower than the modal expansion method by a factor 20–24 minutes as compared to seconds of the modal techniques. Figure 9 provides $E_\theta(\phi = 90^\circ)$ utilizing the modal expansion on the original 81×81 measured points whereas the integral equation has been applied to the central 41×41 points only.

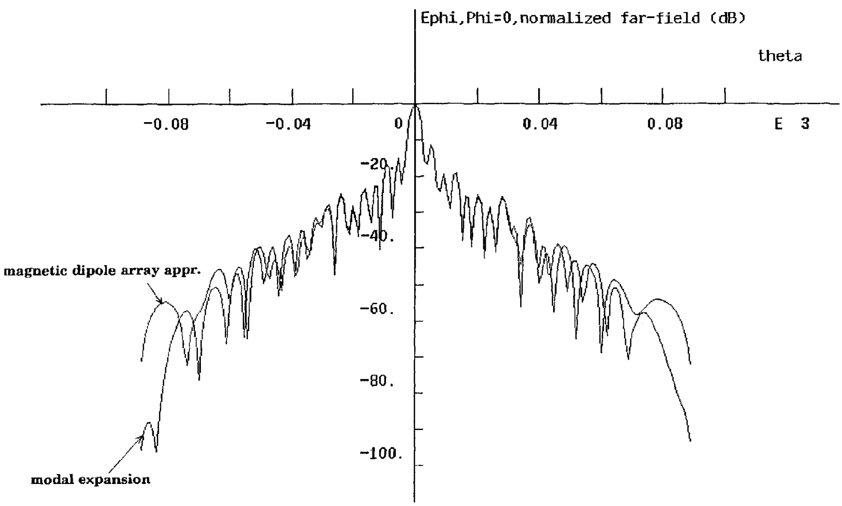

Figure 8. Co-polarization characteristic for $\Phi = 0^\circ$ cut for a 32×32 patch microstrip array using planar modal expansion method (81×81 data points) and equivalent magnetic dipole array approximation (41×41 data points)

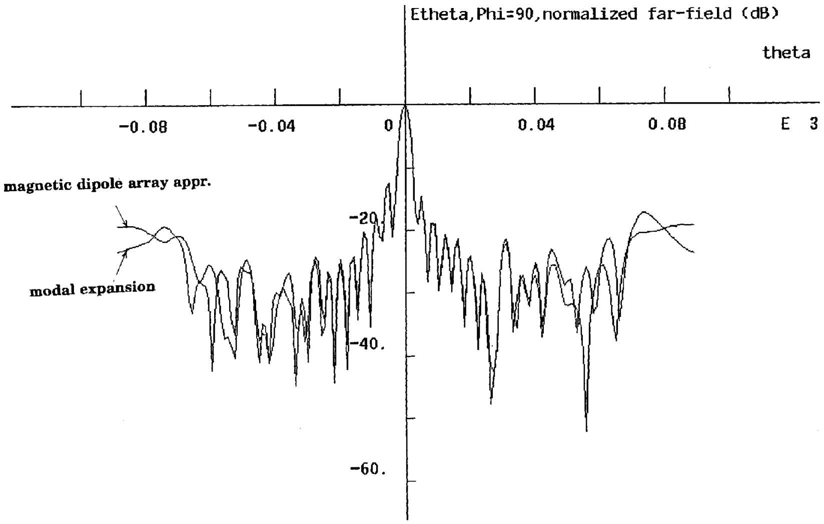

Figure 9. Co-polarization characteristic for $\Phi = 90°$ cut for a 32×32 patch microstrip array using planar modal expansion method (81×81 data points) and equivalent magnetic dipole array approximation (41×41 data points).

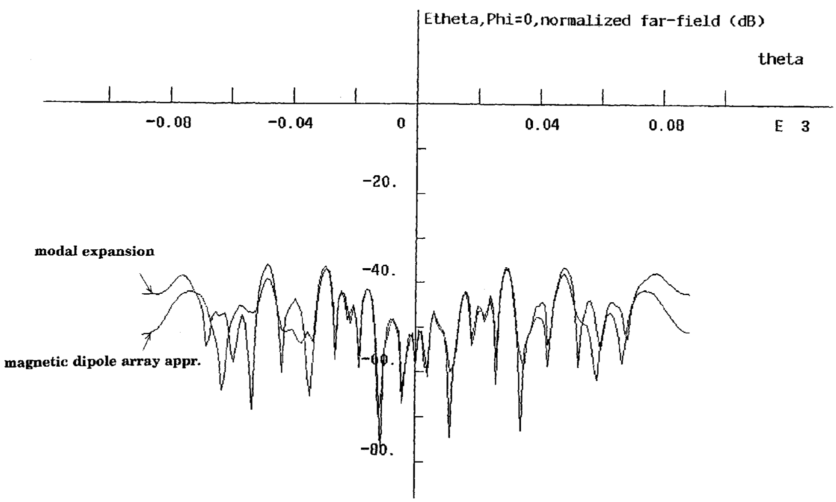

Figure 10. Cross-polarization characteristic for $\Phi = 0°$ cut for a 32×32 patch microstrip array using planar modal expansion method (81×81 data points) and equivalent magnetic dipole array approximation (41×41 data points).

Again, the two curves agree till $\pm\ 40^\circ$ and the agreement is reasonable outside that region. These are the two principal planes co-polar pattern. Next we look at the cross-polar pattern. Figure 10 provides $E_\theta(\phi = 0^\circ)$ utilizing the modal expansion on the 81×81 points and the integral equation approach utilizing 41×41 data points.

Even though the cross-polar pattern is 40 db down, reasonable agreement is seen upto $\pm 40^\circ$. Figure 11 provides $E_\theta\,(\phi = 90^\circ)$ utilizing the modal expansion and the integral equation approach.

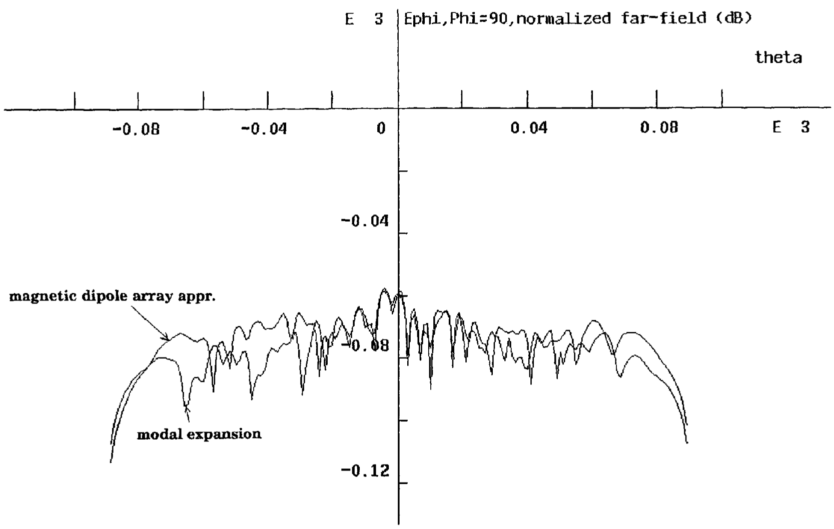

Figure 11. Cross-polarization characteristic for $\Phi = 90^\circ$ cut for a 32×32 patch microstrip array using planar modal expansion method (81×81 data points) and equivalent magnetic dipole array approximation (41×41 data points).

Because this pattern is 60 dB down, the accuracy of both the methods are being compared at a level which corresponds to the noise level. Even then, agreement is reasonable!

Limited experimentation utilizing these two examples (one utilizing synthetic data and other utilizing experimental data) illustrates that it is possible to go beyond the truncation error introduced by the measurement process, by transferring the measurement plane to a source plane containing equivalent sources on a plane closer to the source. It is important to point out that the integral equation method is not creating information that is not there in the measured data. The integral equation method has less truncation error as the processing is different from the conventional modal expansion method. Since the integral equation method is a model-based-parameter-estimation technique, it will always provide higher resolution than the conventional modal expansion method which is FFT based.

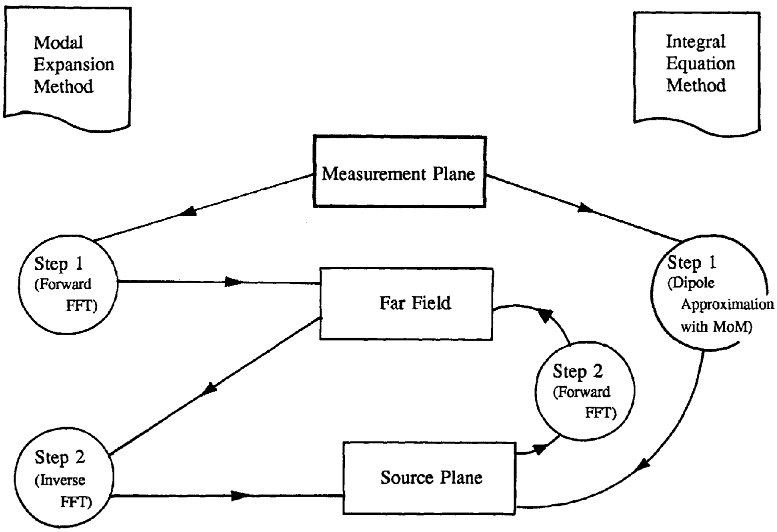

Figure 12. Flow diagrams for the processing of the measured data for the modal expansion method and for the integral equation method.

Let us illustrate this phenomenon by an example. Consider two frequencies $f_2 > f_1 > 0$. Then we know in order to resolve them by the conventional Fourier Processing, we need a data record T which must be greater than $\frac{1}{(f_2 - f_1)}$. This is the principle of uncertainty or the Rayleigh limit as it is popularly called. However, in order to solve for 2 frequencies by a model-based-parameter estimation technique one needs only 4 samples to solve the problem. There are 4 unknowns – 2 amplitudes and 2 frequencies and hence 4 samples should be sufficient to solve the problem. So through this model based parameter estimation technique we are not creating new information, but by assuming a model for the system we are significantly increasing the resolution. This is the motivation of our new approach based on the integral equation technique.

As shown in the block diagram of Fig. 12, we have increased the resolution of the integral equation method over the conventional modal expansion method for processing the identical data set by simply reversing the order of the solution procedure.

It is seen that the modal expansion method first transforms the measured data to the far field by performing a 2D Fourier transform. From the far field, the data is transformed to the source plane by performing a 2D inverse Fourier transform. For the integral equation approach, the measured data is first transformed to the source plane utilizing the dipole approximation for the equivalent sources in the source plane and then solving for their amplitudes by the method of moments. The results are then transformed from the source plane to the far field by performing a 2D-Fourier transform.

Also, it may be possible to significantly reduce the measurement time by as much as 75% if the integral equation approach is selected over the conventional modal expansion method to field same degree of accuracy in the far field. However, the integral equation approach is computationally 20–24 times slower than the modal expansion method.

5. Conclusion

The integral equation approach can provide a reduction of the truncation error caused by performing measurements on a finite plane. This is achieved by transforming and shifting the measured data to a plane which is much closer to the sources. Once the equivalent magnetic currents are found on the source plane, the Fourier techniques can be used to compute the far fields from the magnetic currents. So the price one pays in utilizing the integral equation approach over the modal expansion method is that the integral equation approach takes about 20–25 times more CPU time to produce the far fields for the same number of data points. This estimate has been obtained from the limited cases run in this paper. However, the integral equation approach requires fewer measured data points than the conventional modal expansion method to provide comparable numerical accuracy in the far fields when applied to the same near-field data. So the total measurement time in the integral equation method is less to achieve equivalent numerical accuracy in the far field result compared to the conventional modal expansion method.

Acknowledgment

Part of this research was supported by Rome Laboratory under contract F30602-95-C-0120.

References

1. Paris, D. T., W. M. Leach, Jr., and E. B. Joy, "Basic theory of probe-compensated near-field measurements," *IEEE Trans. on Antennas and Propagation,* Vol. AP-26, No. 3, 373–379, 1978.
2. Joy, E. B., W. M. Leach, Jr., G. P. Rodriguez, and D. T. Paris, "Applications of probe-compensated near-field measurements," *IEEE Trans. on Antennas and Propagation,* Vol. AP-26, No. 3, 379–389, 1978.
3. Yaghjian, A. D., "An overview of near-field antenna measurements," *IEEE Trans. on Antennas and Propagation,* Vol. AP-34, No. 1, 30–45, 1986.
4. Wang, J. J. H., "An examination of the theory for planar near-field measurements," *IEEE Trans. on Antennas and Propagation,* Vol. AP-36, 746–753, 1988.
5. Newell, A. C., "Error analysis techniques for planar near-field measurements," *IEEE Trans. on Antennas and Propagation,* Vol. AP-36, No. 6, 754–768, 1988.
6. Ponnapalli, S., "Near-field to far-field transformation utilizing the conjugate gradient method," *Application of Conjugate Gradient Method in Electromagnetics and Signal Processing,* in PIER 5, T. K. Sarkar, ed. New York, VNU Science Press, Ch. 11, Dec. 1990.
7. Petre, P., and T. K. Sarkar, "Planer near-field to far-field transformation using an equivalent magnetic current approach," *IEEE Trans. of Antennas and Propagation,* 1348–1356, Nov. 1992.
8. Rahmat-Samii, Y., "Surface diagnosis of large reflector antennas using microwave holographic metrology: An iterative approach," *Radio Science,* Vol. 19, 1205–1217, Sept–Oct, 1984.
9. Clemmow, P. C., *The Plane Wave Spectrum Representation of Electromagnetic Fields,* Pergamon Press, 1966.

10. Stubenrauch, Carl, [private communication]
11. Petre, P., and T. K. Sarkar, "Planar near-field to far field transformation using an array of dipole probes," *IEEE Trans. on Antennas and Propagation,* Vol. 42, 534–537, April 1994.